Transmission electron microscope study of polyphase and discordant monazites: Site-specific specimen preparation using the focused ion beam technique

Anne-Magali Seydoux-Guillaume* Institut für Planetologie, Wilhelm-Klemm-Strasse 10, 48149 Münster, Germany
Philippe Goncalves* Université Blaise-Pascal, Laboratoire Magmas et Volcans-CNRS, 5 rue Kessler, 63038 Clermont-Ferrand, France
Richard Wirth GeoForschungsZentrum-Potsdam, Division 4, Telegrafenberg, 14473 Potsdam, Germany
Alexander Deutsch Institut für Planetologie, Wilhelm-Klemm-Strasse 10, 48149 Münster, Germany

ABSTRACT

Electron-microprobe (EMP) U-Th-Pb dating on polyphase and discordant monazites from polymetamorphic granulites of the Andriamena unit (north-central Madagascar) reveals inconsistent chemical ages. To explain these drastic variations, transmission electron microscopy (TEM) foils were prepared directly from thin sections by using the focused ion beam technique. The most important result of the TEM study is the demonstration of the presence of small (~50 nm) Pb-rich domains where large variations in EMP ages occur. We suggest that radiogenic Pb was partially reincorporated in monazite during the recrystallization at 790 Ma. Because the excited volume of EMP is ~4 μm³, U-Th-Pb dating yielded various apparent older ages without geological significance. In addition, TEM analysis of the foils revealed the presence of an ~150-nm-wide amorphous zone along the grain boundary of monazite and its host quartz. This Fe-Si-Al–rich phase may have formed as a result of fluid activity at 500 Ma, and the phase's amorphous state may be due to the irradiation from U and Th decay in the monazite. This demonstrates for the first time the enormous potential of the TEM investigations on site-specific specimens prepared with the focused ion beam technique for the interpretation of geochronological data.

Keywords: monazite, discordance, focused ion beam, transmission electron microscopy, U-Th-Pb ages, Madagascar.

INTRODUCTION

In polymetamorphic terranes, most studies combining electron-microprobe (EMP) U-Th-Pb dating (EMP chemical ages) with conventional isotopic techniques have shown that monazites behave as a closed system (Crowley and Ghent, 1999; Terry et al., 2000; Williams and Jercinovic, 2002). Other authors, however, reported large variations in EMP ages, inconsistent with discrete episodic growth of monazite (Montel et al., 1996; Braun et al., 1998; Cocherie et al., 1998; Catlos et al., 2002; Goncalves, 2002; Fig. 1). Two explanations are given for this observation: (1) partial Pb loss from monazite by diffusion or leaching, implying that the EMP age data represent minimum ages, or (2) overlapping measurement of different age domains by the EMP, resulting in mixed apparent ages. The aim of this study was to elucidate the reason for inconsistent EMP ages, reported for polyphase monazites from ultrahigh-temperature (UHT) granulites of north-central Madagascar (Goncalves, 2002; Paquette et al., 2003). This goal was achieved by using transmission electron microscopy (TEM).

*E-mail: Seydoux-Guillaume—seydoux@uni-muenster.de. Present address: Goncalves—Geosciences Department, University of Massachusetts, Morrill Science Center, 611 North Pleasant Street, Amherst, Massachusetts 01003-9297, USA.

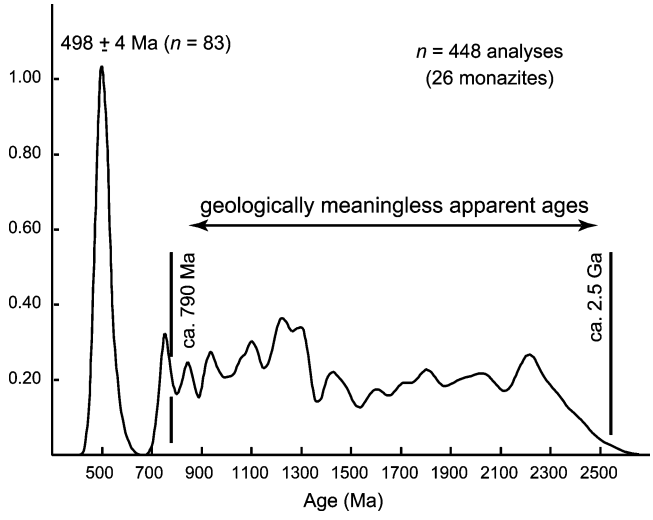

Figure 1. Weighted histogram of 448 electron microprobe (EMP) chemical U-Th-Pb ages for 26 monazites included in garnet, quartz, and coronitic textures. 2.5 Ga and 790 Ma ages were derived from isotope dilution–thermal ionization mass spectrometer data; 500 Ma age is from EMP data on monazite overgrowths. Note continuous range of EMP ages between 2500 and 790 Ma (after Goncalves, 2002).

DESCRIPTION OF THE PROBLEM

The investigated monazites record three distinct episodes of crystallization: at 2.5 Ga under UHT conditions, ca. 790 Ma, related to hydration and retrograde metamorphism of the UHT assemblages, and at 500 Ma, during a growth episode due to late fluid circulation under low amphibolite facies conditions (Goncalves, 2002). The succession of events was revealed by textural studies, EMP chemical dating (Fig. 2), and isotope dilution–thermal ionization mass spectrometer (ID-TIMS) dating of extracted selected grains. The ID-TIMS dating yielded discordant ages defining a mixing array involving the 2500, 790, and 500 Ma age components, and a geologically meaningless lower intercept ca. 580 Ma (Goncalves, 2002, Paquette et al., 2003).

The EMP ages, however, do not show a simple trimodal distribution reflecting the geological events at 2500, 790, and 500 Ma (Fig. 1). On the contrary, most grains are characterized by (1) meaningless apparent ages ranging continuously between 2500 and 790 Ma and (2) a very well defined unimodal population clustering at 500 Ma (Fig. 1). In addition, age dispersions are observed within single monazite grains. It is noteworthy that the grain ages scatter irregularly. In contrast, areas with an apparent age of 500 Ma systematically form small overgrowths, or internal domains close to small quartz inclusions, orthoamphibole, biotite, or cordierite.

Two questions remained unanswered after this combined in situ dating: what is the reason for largely varying apparent ages in a single monazite grain, and what is the difference between the well-defined 500 Ma overgrowths

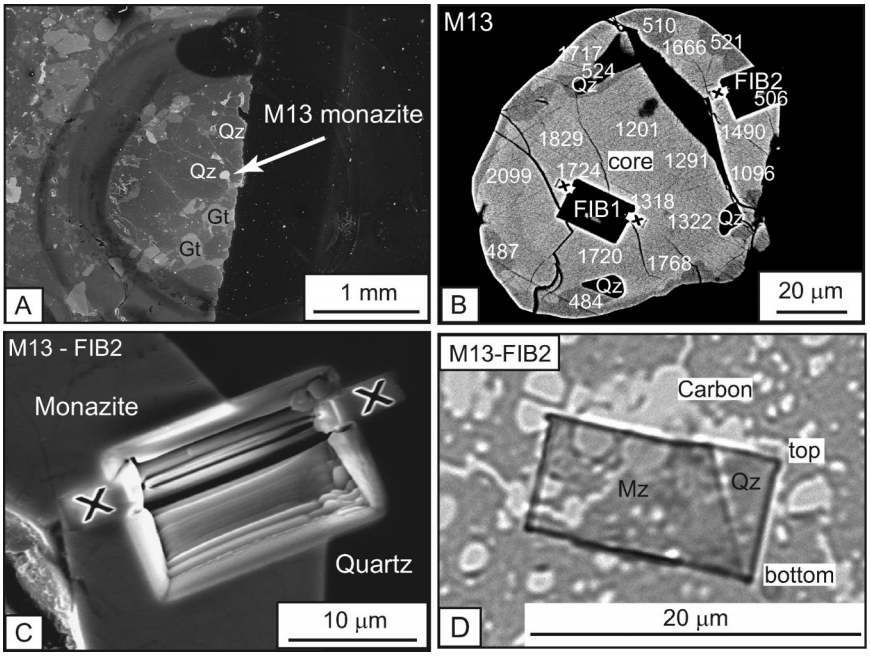

Figure 2. Preparation of transmission electron microscopy (TEM) foils from monazite M13 using focused ion beam (FIB) technique. A: Backscattered-electron (BSE) image of thin section with monazite M13 embedded in quartz (Qz) with associated garnet (Gt). B: Close-up BSE image of monazite M13. Bright areas (core) formed at 790 Ma; dark areas are 500 Ma overgrowths. Numbers are U-Th-Pb ages in Ma obtained by electron microprobe. C: Secondary-electron image of FIB milled trench with TEM foil removed. Foil was milled perpendicular to image plane along trace marked by crosses. D: Optical micrograph in transmitted light of TEM-ready FIB foil on perforated carbon film on copper grid. Foil dimensions are 15 μm × 7 μm × 130 nm.

and the domains showing geologically meaningless ages? Nanometer-scale investigations to solve these problems required preparation of TEM foils—ultrathin, ultrasmall tabular sections—from defined areas in monazite grains that have been dated by the EMP technique (Figs. 2B and 3A). For this purpose, we applied the focused ion beam (FIB) milling technique.

METHODS

Focused Ion Beam (FIB) Technique

The FIB preparation technique is designed to produce site-specific TEM foils, ~15–20 μm × 10–15 μm, and ~100 nm thick (for technical details, see Overwijk et al., 1993; Young, 1997; Roberts et al., 2001). Milling occurs by using gallium ions accelerated to 30 keV. Carbon coating of the TEM-ready foil is not necessary, because it rests on carbon foil. The FIB allows cutting a TEM-ready foil in a section from a well-defined area such as mineral boundary, without preferential thinning or production of artifacts (e.g., Fig. 4D). Homogeneous sample thickness is very favorable, especially for acquisition of elemental maps or line scans (Figs. 3C and 3D). The TEM foil is cut perpendicular to the surface of the sample (Figs. 2C and 2D), allowing the gathering of information with respect to the depth of the specimen. In the current context, this aspect is particularly useful for testing the reliability of specific EMP age data.

The site-specific specimens for this study were prepared with the FEI FIB200 instrument at the GeoForschungsZentrum (GFZ)-Potsdam. Figure 2 illustrates subsequent stages of the preparation.

Transmission Electron Microscope (TEM)

TEM studies were carried out with the Philips CM200 TEM at the GFZ-Potsdam, and the JEOL 3010 TEM of the Interdisciplinary Center for Electron Microscopy and Microanalysis (ICEM), University of Münster. The JEOL 3010, operating at 300 kV, was used for conventional TEM. The Philips CM200, equipped with an energy-dispersive X-ray analyzer (EDAX) with an ultrathin window, was used for energy-dispersive X-ray (EDX) analysis and EDX mapping. Acceleration voltage was 200 kV, and the electron source was a LaB_6 filament. Point analyses were carried out with a spot size of ~4 nm; the counting time for EDX point analysis was 200 s, and 45 ms per step in EDX mapping.

SAMPLE DESCRIPTION

Two monazite grains (M13 and M26) were selected for the TEM study. (For simplicity we relabeled these grains, labeled by Goncalves [2002] M13′ and M26″.) These monazites are representative for the whole population because they display the typical bimodal age distribution. Both grains were originally located in polygonal recrystallized quartz within the rock matrix. The 110 μm monazite M26 displays a chemically distinct core, surrounded by a homogeneous rim and isolated small overgrowths (Fig. 3A). The distributions of EMP age data in core and rim are similar, scattering continuously from 1805 to 911 Ma (Fig. 3A). In contrast, overgrowths yielded systematically younger dates, ca. 500 Ma. As shown in the backscattered-electron (BSE) image (Fig. 2B), the 160 μm monazite M13 revealed only two domains: (1) a large core and (2) darker areas located at the rim and at the contact with quartz inclusions. These areas with an average age of 504 ± 15 Ma are interpreted as younger recrystallized domains. The EMP ages in the core range from 2099 to 1096 Ma.

On the basis of these EMP ages and ID-TIMS results, Goncalves (2002) interpreted the cores of M13 and M26 as 2.5 Ga monazites, which underwent partial Pb loss during the 790 Ma event. Goncalves further suggested that the rim on monazite M26 was formed by dissolution followed by precipitation at 790 Ma, despite the older ages obtained by EMP. The overgrowth crystallized ca. 500 Ma.

NANOSCALE INVESTIGATIONS OF MONAZITE WITH COMPLEX AGES

In monazite M13, the TEM foil FIB1 was extracted from the old core, and foil FIB2 includes the core and the dark area giving consistent 500 Ma ages (Fig. 2B). In M26, foil FIB1 covers core and rim (Fig. 3A).

Structural State

Bright-field (BF) images of all domains in these monazites consistently show a typical pattern, i.e., mottled diffraction contrasts due to the presence of distorted volumes (Fig. 4B; cf. Black et al., 1984; Seydoux-Guillaume et al., 2002a). These lattice defects are produced by self-irradiation due to the α-decay of U and Th. An important observation is the lack of significant difference in defect concentration in the 500 Ma domains and the old cores of both monazites. Note the presence of mottled diffraction contrasts in quartz as well; these are also due to lattice defects, which are probably caused by irradiation related to U and Th decay in the monazite (Fig. 4D).

Nanometer-Sized Pb-Rich Domains

Many ~50-nm-sized domains were observed in the core and the rim of monazite M26 (Fig. 3B) and in the core of monazite M13 (Fig. 4C). Figure 3D shows EDX mapping results for Pb in M26. The lead is not homogeneously distributed (Fig. 3D): the dark domains labeled 2 and 3 and one fluid inclusion (Fig. 3B) are enriched in Pb (Fig. 3D). The EDX point

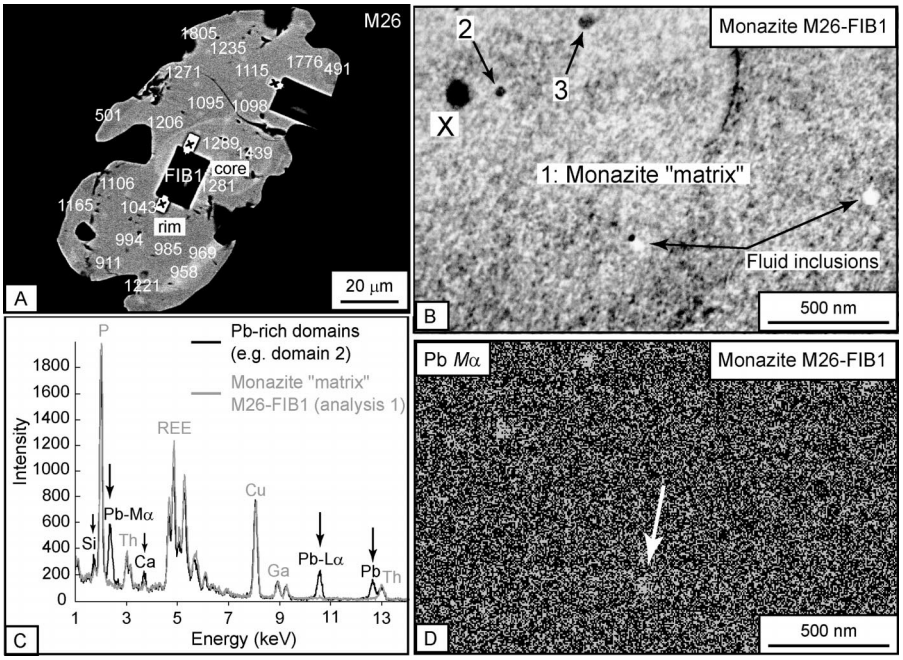

Figure 3. Energy-dispersive X-ray (EDX) analysis of monazite M26. A: Backscattered-electron (BSE) image. Foil FIB1 covers core and slightly darker rim. Numbers correspond to electron microprobe (EMP) ages. B: Bright-field (BF) transmission electron microscope (TEM) image of monazite core in FIB1 foil (see A). Note dark domains 2 and 3 and two fluid inclusions. Dark domain X corresponds to contamination of foil with Ga ions dispersed during focused ion beam (FIB) milling. Mottled diffraction contrasts are due to distorted volumes in monazite lattice (cf. Fig. 4B). C: Overlay of analysis 1 of monazite matrix and representative EDX analysis of dark domain in B is reported. As TEM foil has fairly uniform thickness, analyzed volumes are same, allowing direct comparison of two analyses. Compared to monazite matrix, dark domains are very enriched in Pb and, to lesser extent, in Ca and Si. Cu and Ga are preparation artifacts. REE—rare earth elements. D: EDX map of Pb*Mα* for area shown in B. Domains 2 and 3 and one fluid inclusion (arrow) are enriched in Pb (brighter in this image) compared to monazite matrix.

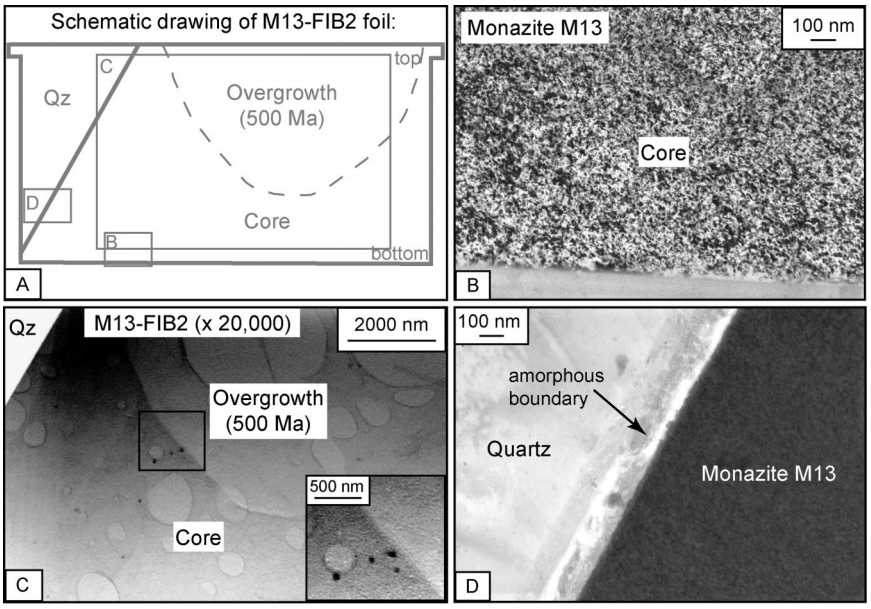

Figure 4. Transmission electron microscope (TEM) images of FIB2 foil, monazite M13. A: Schematic drawing shows different zones and locations of details given in B–D. B: Bright-field (BF) image of part of core region, showing mottled diffraction contrasts. C: BF image showing monazite, old core, with largely varying U-Th-Pb ages, and young overgrowth, together with host mineral, quartz (Qz). Bright circles correspond to holes in perforated carbon supporting TEM foil. Note small Pb-rich domains in core (dark areas in rectangle; see enlargement on lower right). D: BF image of boundary between quartz and monazite. Note presence of ~150-nm-wide amorphous phase and mottled diffraction contrasts in quartz due to lattice defects.

analysis (Fig. 3C) corroborates this observation: compared to the monazite matrix, the inclusions are considerably enriched in Pb and, to a lesser extent, in Ca and Si. Because the electron beam of the TEM covers both inclusions and monazite matrix, the precise chemical composition of the Pb-rich domains could not be determined. The core of monazite M13 yields similar results. In contrast, Pb-rich domains seem to be absent in the 500 Ma overgrowths (Fig. 4).

Phase Boundary Between Monazite and Quartz

The FIB technique permits analysis of defined, few-nanometers-small areas and inclusions, which usually are destroyed during conventional TEM preparation methods (ion milling). This fundamental advantage helped to study the phase boundary between monazite and quartz in monazite M13 (TEM foil FIB2; Figs. 2D, 4A, 4C, and 4D). At the micrometer scale (Fig. 2C), this boundary looks very narrow and sharp. At the nanometer scale, however, the interface is ~150 nm wide. It consists of an amorphous phase (Fig. 4D), which according to EDX analysis, is composed of O, Fe, and Si in approximately the same proportions, and, to a lesser extent, Al.

DISCUSSION AND IMPLICATIONS

α-Decay Damages

Goncalves (2002) explained the range in apparent ages by partial Pb loss from 2.5 Ga monazites. Clearly, in such old monazites, self-irradiation due to α-decay from U and Th must have induced more defects than that in the 500 Ma overgrowths, and Pb is probably much more mobile in such a distorted lattice than in a perfect one (Cherniak, 1993). In the present case, however, zones with different ages have a similar concentration of defects, making enhanced Pb mobility due to different structural states highly improbable.

Implication of the Presence of Pb-Rich Inclusions

The occurrence of nanometer-sized Pb-rich domains in monazites has strong implications for EMP dating. The main advantage of EMP dating is the high spatial resolution: at conventional analytical conditions, the excited volume is ~4 μm^3, which is very small compared to single-grain U-Pb ID-TIMS dating (Montel et al., 1996; Paquette and Pin, 2001), yet relatively large on the TEM scale. By using the EMP dating technique, it is not possible to exclude nanometer-sized Pb-rich domains from the analysis. In chemical dating, all Pb is considered to be of in situ radiogenic origin; hence, inclusion of Pb-rich domains in the analysis yields an older apparent age.

On the basis of these arguments, the interpretation of Goncalves (2002)—that the cores

of both M26 and M13 grain are partially reset 2.5 Ga monazites—is reconsidered. We now assume that the 2.5 Ga monazites dissolved and recrystallized at 790 Ma. All apparent ages older than 790 Ma result from mixing of the 790 Ma domains with Pb-rich domains, which contain inherited radiogenic Pb from the 2.5 Ga monazite. This surprising outcome emphasizes that special care must be taken in interpreting chemical zoning visible in BSE images in terms of different monazite generations.

The nature of the Pb-rich domains is not understood. They could (1) be a pure Pb-Ca-Si-O phase like margarosanite ($Ca_2PbSi_3O_9$), (2) represent material that crystallized in fluid inclusions (Fig. 3B), or (3) be a local domain in the monazite structure, high in lead, like the brabantite [$PbTh(PO_4)_2$] experimentally synthesized by Montel et al. (2002).

Goncalves (2002) documented some 2.5 Ga monazites that survived the 790 Ma event as inclusions in garnet. In the rock matrix, however, these old monazites were probably affected by dissolution followed by precipitation at 790 Ma, when cordierite + orthoamphibole + biotite formed at the expense of garnet + quartz. The newly formed 790 Ma monazite incorporated radiogenic Pb, previously released during the dissolution of the 2.5 Ga monazite. The EMP U-Th-Pb ages indicate a heterogeneous distribution of this old radiogenic lead. Generally, incorporation of Pb depends on its distribution coefficient between the different phases involved in the reaction. For example, Pb would be concentrated in fluids relative to monazite and in monazite relative to garnet or quartz. In hydrothermal experiments, monazite releases or incorporates Pb from a fluid depending on the relative concentrations and the external conditions (Seydoux-Guillaume et al., 2002b). Although we cannot exclude incorporation of the old radiogenic Pb in the form of brabantite into the monazite structure, we prefer the interpretation that this Pb is concentrated in nanometer-sized Pb-rich domains. Regardless of the precise location of the radiogenic Pb in the monazite, the important implication for dating is the fact that domains of unsupported Pb exist in monazite.

Role of the Fluid in Resetting Monazites

The boundary between monazite and its host quartz is not a sharp contact between pure crystalline phases, but lined with an amorphous phase (Fig. 4D), the exact nature of which is unknown. We propose this phase to be an indicator of fluid activity. It could be a low-temperature phase (a clay mineral) or an amphibolite facies mineral, that later became metamict by irradiation from adjacent monazite. In the thin section shown in Figure 2, monazite M13 is included in quartz, but this grain was not completely armored; overgrowths on the monazite record the 500 Ma event (Fig. 2B). We emphasize that all these young overgrowths are localized either at the monazite-quartz interface or close to quartz inclusions (e.g., the 524 and 484 Ma domains in Fig. 2B). We tentatively conclude that the event that yielded these monazite overgrowths took place ca. 500 Ma during late fluid circulation under low amphibolite facies conditions (Goncalves, 2002). The boundary between monazite and quartz acted as the channel for fluid circulation. Our observations confirm the major role of fluids in the resetting of monazites (Teufel and Heinrich, 1997; Seydoux-Guillaume et al., 2002a; Villa, 2002).

CONCLUSIONS

In U-Th-Pb dating of minerals from polymetamorphic terranes, the combined use of different methods is extremely useful. Possible analytical techniques include single-grain ID-TIMS and EMP U-Th-Pb dating of petrographically and chemically characterized crystals as well as TEM observations (Seydoux-Guillaume et al., 2002a; Villa, 2002). The behavior of U-Th-Pb systems in minerals during metamorphism at the single-grain scale is currently poorly understood. For example, Romer and Rötzler (2003) provided an example of a titanite that inherited the radiogenic signature of its precursor mineral rutile. In this, the TEM study of site-specific FIB foils resulted in a new understanding of EMP ages for monazites from a polymetamorphic terrane: the range in apparent ages is not the consequence of partial Pb loss, a process commonly used for interpretation, but instead is due to the incorporation of various amounts of radiogenic Pb during recrystallization of the monazites. The development of more sophisticated, more precise geochronologic techniques requires a strong effort in the understanding of what really happens to the isotopic systems in dated minerals.

ACKNOWLEDGMENTS

This work was supported by German Science Foundation (DFG) grant De 401/18-1 to Deutsch. We appreciate technical assistance by F. Bartschat and T. Grund. C. Nicollet is acknowledged for providing the unusual samples. We thank J.M. Montel and M.L. Williams for reviewing an early draft of the manuscript, and J. Connelly and D. Waters for their constructive formal reviews.

REFERENCES CITED

Black, L.P., Fitzgerald, F.D., and Harley, S.L., 1984, Pb isotopic composition, colour, and microstructure of monazites from a polymetamorphic rock in Antarctica: Contributions to Mineralogy and Petrology, v. 85, p. 141–181.

Braun, I., Montel, J.M., and Nicollet, C., 1998, Electron microprobe dating of monazite from high-grade gneisses and pegmatites of the Kerala Khondalite belt, southern India: Chemical Geology, v. 146, p. 65–85.

Catlos, E.J., Gilley, L.D., and Harrison, T.M., 2002, Interpretation of monazite ages obtained via in situ analysis: Chemical Geology, v. 188, p. 193–215.

Cherniak, D.J., 1993, Lead diffusion in titanite and preliminary results on the effect of radiation damage on Pb transport: Chemical Geology, v. 110, p. 177–194.

Cocherie, A., Legendre, O., Peucat, J.J., and Kouamelan, A.N., 1998, Geochronology of polygenetic monazites constrained by in situ electron microprobe Th–U–total lead determination: Implications for lead behaviour in monazite: Geochimica et Cosmochimica Acta, v. 62, p. 2475–2497.

Crowley, J.L., and Ghent, E.D., 1999, An electron microprobe study of the U-Th-Pb systematics of metamorphosed monazite: The role of Pb diffusion versus overgrowth and recrystallisation: Chemical Geology, v. 157, p. 285–302.

Goncalves, P., 2002, Pétrologie et géochronologie des granulites de ultra-hautes temperatures de l'unité basique d'Andriamena (Centre-Nord Madagascar): Apport de la géochronologie in situ U-Th-Pb à l'interprétation des trajets *P-T* [thèse de doctorat]: Clermont-Ferrand, France, Université Blaise-Pascal, 319 p.

Montel, J.M., Foret, S., Veschambre, M., Nicollet, C., and Provost, A., 1996, Electron microprobe dating of monazite: Chemical Geology, v. 131, p. 37–53.

Montel, J.M., Devidal, J.L., and Avignant, D., 2002, X-ray diffraction study of brabantite-monazite solid solutions: Chemical Geology, v. 191, p. 89–104.

Overwijk, M.H.F., van den Heuvel, F.C., and Bulle-Lieuwma, C.W.T., 1993, Novel scheme for the preparation of transmission electron microscopy specimens with a focused ion beam: Journal of Vacuum Science and Technology, v. 11, p. 202.

Paquette, J.L., and Pin, C., 2001, A new miniaturized extraction chromatography method for precise U-Pb zircon geochronology: Chemical Geology, v. 176, p. 311–319.

Paquette, J.L., Goncalves, P., Devouard, B., and Nicollet, C., 2003, In situ ID-TIMS U-Pb dating of single monazites: A new method to unravel complex poly-metamorphic evolutions. Application to the UHT granulites of Andriamena (north-central Madagascar): Contributions to Mineralogy and Petrology (in press).

Roberts, S., McCaffrey, J., Giannuzzi, L., Stevie, F., and Zaluzec, N., 2001, Advanced techniques in TEM specimen preparation, *in* Xiao-Feng Zhang and Ze Zhang, eds., Progress in transmission electron microscopy, Volume 1: Springer Series in Surface Sciences, v. 38, p. 336–342.

Romer, R.L., and Rötzler, J., 2003, Effect of metamorphic reaction history on the U-Pb dating of titanite: Geological Society [London] Special Publication (in press).

Seydoux-Guillaume, A.M., Wirth, R., Nasdala, L., Gottschalk, M., Montel, J.M., and Heinrich, W., 2002a, An XRD, TEM and Raman study of experimentally annealed natural monazite: Physics and Chemistry of Minerals, v. 29, p. 240–253.

Seydoux-Guillaume, A.M., Paquette, J.L., Wiedenbeck, M., Montel, J.M., and Heinrich, W., 2002b, Experimental resetting of the U-Th-Pb system in monazite: Chemical Geology, v. 191, p. 165–181.

Terry, M.P., Robinson, P., Hamilton, M.A., and Jercinovic, M.J., 2000, Monazite geochronology of UHP and HP metamorphism, deformation, and exhumation, Nordoyane, Western Gneiss region, Norway: American Mineralogist, v. 85, p. 1651–1664.

Teufel, S., and Heinrich, W., 1997, Partial resetting of the U-Pb isotope system in monazite through hydrothermal experiments: An SEM and U-Pb isotope study: Chemical Geology, v. 137, p. 273–281.

Villa, I., 2002, Where is geochronology going? Alteration and mineral mixtures: Geochimica et Cosmochimica Acta, v. 66, no. S1, p. A807.

Williams, M.L., and Jercinovic, M.J., 2002, Microprobe monazite geochronology: Putting absolute time into microstructural analysis: Journal of Structural Geology, v. 24, p. 1013–1028.

Young, R.J., 1997, Application of the focused ion beam in materials characterization and failure analysis: Microstructural Science, v. 25, p. 491–496.

Manuscript received 12 February 2003
Revised manuscript received 18 July 2003
Manuscript accepted 29 July 2003

Printed in USA